PNAS BRIEF REPORT | BIOPHYSICS AND COMPUTATIONAL BIOLOGY OPEN ACCESS

AcrIE7 inhibits the CRISPR-Cas system by directly binding to the R-loop single-stranded DNA

Do Yeon Kim[a,1], So Yeon Lee[a,1], Hyun Ji Ha[a,1], and Hyun Ho Park[a,2]

Edited by Eugene Koonin, National Institutes of Health, Bethesda, MD; received November 22, 2024; accepted March 5, 2025

The CRISPR-Cas system is a well-known adaptive immune system in bacteria, and a prominent mechanism for evading this immunity involves anti-CRISPR (Acr) proteins, which employ various methods to neutralize the CRISPR-Cas system. In this study, using structural and biochemical analyses, we revealed that AcrIE7 binds to the single-stranded DNA in the R-loop formed when Cascade encounters the target DNA, thereby preventing Cas3 from cleaving the DNA. This represents a different inhibition strategy distinct from previously reported Acr mechanisms and offers insights into CRISPR-Cas inhibition.

anti-CRISPR | AcrIE7 | adaptive immunity | CRISPR-Cas system | crystal structure

In bacteria and archaea, CRISPR loci and the associated CRISPR-associated (Cas) proteins form a defense system (CRISPR-Cas) against invading nucleic acids (1). One of the key areas of research in CRISPR-Cas biology is the regulation of these systems, which includes anti-CRISPR (Acr) proteins (2). Acr proteins are small, naturally occurring inhibitors produced by bacteriophages to counteract the CRISPR-Cas immune defense (3). By binding to and inhibiting specific Cas proteins, Acrs help phages evade destruction, establishing a dynamic evolutionary arms race between bacterial defense and phage countermeasures (2). To date, several classes of Acr proteins have been identified, each displaying distinct inhibitory mechanisms (2, 4, 5). Acrs inhibit CRISPR-Cas systems by blocking DNA/RNA binding (AcrIIA2) (6), preventing guide RNA association (AcrIIA1) (7), disrupting complex assembly (AcrIF25) (8), or recruiting host proteases for degradation (AcrIIC3) (9).

AcrIE7 is one such anti-CRISPR protein that inhibits the type I-E CRISPR-Cas system (10). This Acr was identified as one of the seven novel genes located upstream of the aca1 gene in the *Pseudomonas* genome (10). The type I-E CRISPR-Cas system employs the CRISPR-associated complex for antiviral defense (Cascade complex) to identify and degrade foreign DNA, with the nuclease-helicase Cas3 being essential for DNA degradation (10). The two main mechanisms by which the AcrIE family inhibits the CRISPR system are well known: the first involves direct binding to the Cascade complex, as seen with AcrIE2 and AcrIE3 (11), and the second involves binding to Cas3 to inhibit its activity, as seen with AcrIE1 (12). However, the inhibition mechanisms of other AcrIE family members, including AcrIE7, remain unknown. Therefore, in this study, we aimed to determine the mechanism by which AcrIE7 inhibits the CRISPR-Cas system.

Results and Discussion

To investigate how AcrIE7 inhibits the CRISPR-Cas system, we determined its structure, revealing a seven-helix helical bundle fold (Fig. 1 *A* and *B*). Significant differences were observed between the experimentally determined structure and the AlphaFolds (AF2 and AF3) predicted model (Fig. 1 *C* and *D*). AcrIE7 is a rare case wherein the experimental structure deviates substantially from the predicted model. DALI analysis identified structural homologs with low similarity (Fig. 1*E*), suggesting that AcrIE7 represents a unique fold.

We analyzed the surface electrostatic properties of AcrIE7 and found that two distinct basic patches were clearly identified (Fig. 1*F*). As basic patches can be used for nucleic acid binding, we analyzed whether AcrIE7 directly binds to either double-stranded DNA (dsDNA) or single-stranded DNA (ssDNA) using an electrophoretic mobility shift assay (EMSA). The results show that AcrIE7 does not bind to dsDNA but does bind to ssDNA, resulting in the formation of an AcrIE7/ssDNA complex band (Fig. 1*G*). Interestingly, AcrIE7 itself was stained with the nucleic acid dye (Fig. 1*G*). The MALS analysis revealed a measured molecular weight of 13.9 kDa, which was close to the calculated molecular weight of AcrIE7, 13.0 kDa (Fig. 1*H*). Based on these results, we confirmed that AcrIE7

Author affiliations: [a]Department of Global Innovative Drugs, College of Pharmacy, Chung-Ang University, Seoul 06974, Republic of Korea

Author contributions: H.H.P. designed research, D.Y.K., S.Y.L., and H.J.H. performed research; D.Y.K., S.Y.L., H.J.H., and H.H.P. analyzed data; and D.Y.K., S.Y.L., H.J.H., and H.H.P. wrote the paper.

The authors declare no competing interest.

[1]D.Y.K., S.Y.L., and H.J.H. contributed equally to this work.

[2]To whom correspondence may be addressed. Email: xrayleox@cau.ac.kr.

This article contains supporting information online at https://www.pnas.org/lookup/suppl/doi:10.1073/pnas.2423205122/-/DCSupplemental.

Published April 3, 2025.

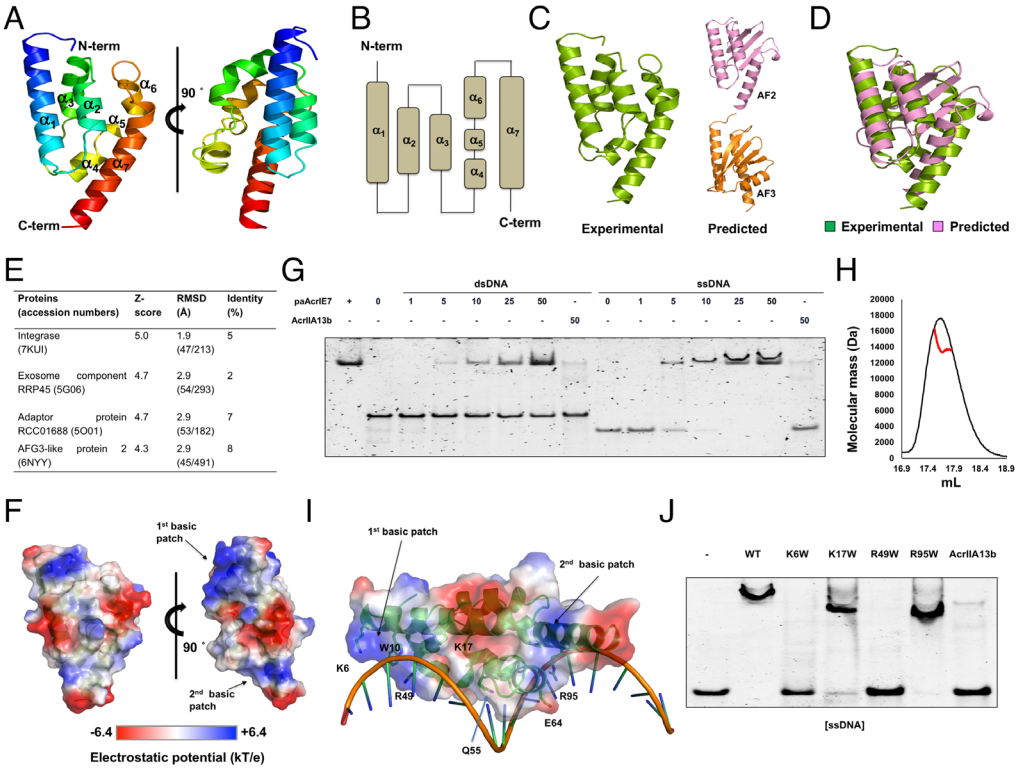

Fig. 1. The overall structure and ssDNA binding capability of AcrIE7. (*A*) A ribbon diagram of AcrIE7. (*B*) Topology diagram of the AcrIE7 structure. (*C* and *D*) Comparison of AcrIE7 crystal structure with AlphaFold2 (AF2) and AlphaFold3 (AF3) prediction. (*E*) Summary of the DALI search results. (*F*) Electrostatic surface representation of AcrIE7. (*G*) EMSA for detecting the binding of AcrIE7 with nucleic acids. (*H*) MALS profile from the SEC peak (*I*) Model of the AcrIE7/ssDNA complex. (*J*) EMSA to detect the interaction between various AcrIE7 mutants and ssDNA.

exists as a monomer in solution. Therefore, we conclude that AcrIE7 is a monomeric ssDNA-binding protein.

To analyze AcrIE7–ssDNA binding, we performed HDOCK docking (Fig. 1*I*), identifying two basic patches potentially involved in ssDNA binding. To validate this model, we mutated key residues to tryptophan and assessed binding via EMSA. The results showed that the wild-type AcrIE7 clearly bound to ssDNA. In contrast, the negative control AcrIIA13b, which does not bind ssDNA (13), and the mutants K6W and R49W did not induce an upper shift in the ssDNA band, indicating that these mutants could not bind to ssDNA (Fig. 1*J*). For the K17W and R95W mutants, an upper shift in the DNA-binding band was observed; however, the positions of these bands differed from those of the wild-type AcrIE7 (Fig. 1*J*). Based on these results, we conclude that the first basic patch, consisting of K6 and R49, plays a crucial role in the binding of AcrIE7 to ssDNA.

To investigate how AcrIE7 binds to ssDNA and potentially inhibits the CRISPR-Cas system, we synthesized FAM-labeled ssDNA (Fig. 2*A*). As reported in previous studies, ssDNA is efficiently cleaved by Cas3 (14). In our system, FAM-labeled ssDNA was cleaved in the presence of Cas3 (Fig. 2*B*) and effectively bound to AcrIE7 (Fig. 2*C*). To test whether AcrIE7 affects Cas3-mediated ssDNA cleavage, we examined cleavage in its presence. When AcrIE7 was preincubated or added simultaneously with Cas3, ssDNA cleavage was inhibited (Fig. 2*D*). However, inhibition alone did not confirm direct ssDNA binding by AcrIE7, as no upper shift was observed in PAGE. We hypothesized that SDS in the stop solution disrupted AcrIE7–ssDNA binding, leaving only unbound, noncleaved ssDNA detectable. Repeating the assay without SDS revealed a concentration-dependent AcrIE7–ssDNA complex band, confirming direct binding and protection from Cas3 cleavage (Fig. 2*E*). To verify that ssDNA binding is essential for inhibition, we tested nonbinding mutants (K6W, R49W). These mutants failed or showed reduced ability to inhibit Cas3-mediated cleavage (Fig. 2*F*). These findings confirm that AcrIE7 inhibits Cas3 by directly binding to ssDNA.

Finally, we investigated whether AcrIE7 could inhibit NTS cleavage in the presence of the complete CRISPR-Cas system, including the Cascade. For this experiment, we synthesized FAM-labeled NTS and unlabeled TS, then annealed them to produce dsDNA with fluorescence on NTS only (Fig. 2*G*). As AcrIC and AcrIE often inhibit both Type I-C and Type I-E CRISPR-Cas systems (15), we used the available Type I-C Cascade in this study. We first confirmed that in the presence of the Cascade alone, the crRNA-R-loop was formed between the TS and NTS of dsDNA. The small size of our 42-bp TS/NTS dsDNA led to partial separation of the TS and NTS, resulting in visible labeled NTS ssDNA (Fig. 2*H*). When Cas3 was added, the NTS ssDNA band weakened due to cleavage, but AcrIE7 inhibited cleavage in a concentration-dependent manner (Fig. 2*H*). These results indicate that AcrIE7 binds NTS ssDNA generated by Cascade and prevents its cleavage by Cas3 within the complete CRISPR-Cas system. Finally, we tested mutants with reduced ssDNA-binding affinity. As expected, their ability to protect NTS ssDNA was significantly lower than that of wild-type AcrIE7 (Fig. 2*I*). These results allow us to suggest that AcrIE7 might bind to NTS ssDNA generated by R-loop formation in the CRISPR-Cas system, thereby inhibiting Cas3 activity and functioning as an anti-CRISPR protein (Fig. 2*J*). If AcrIE7 inhibits by binding to the R-loop ssDNA, the question remains as to how it can

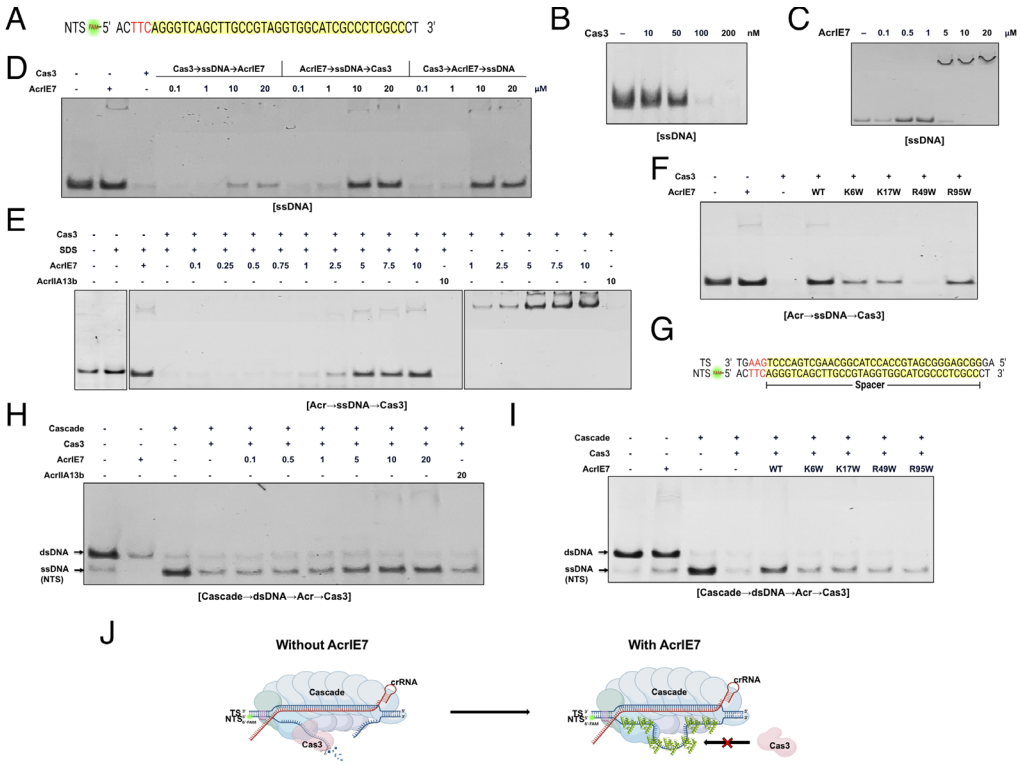

Fig. 2. AcrIE7 inhibits the CRISPR-Cas system by directly binding to R-loop single-strand DNA. (*A*) Sequence of the FAM-labeled NTS used as ssDNA. Red color and yellow highlight indicate the PAM and spacer sequence, respectively. (*B*) Cas3 activity assay. (*C*) Representative EMSA with AcrIE7 using FAM-labeled ssDNA as a substrate. (*D*) In vitro AcrIE7 activity assay in the absence of Cascade. (*E*) The same experiment as in (*D*), including reaction samples with SDS omitted from the stop solution. (*F*) In vitro AcrIE7 activity assay in the absence of Cascade with the indicated AcrIE7 mutants using ssDNA as the substrate. (*G*) Sequence of NTS-labeled dsDNA. (*H*) In vitro AcrIE7 activity assay in the presence of Cascade. (*I*) In vitro AcrIE7 activity assay in the presence of Cascade with the indicated AcrIE7 mutants using dsDNA as a substrate. (*J*) Tentative model for AcrIE7-based inhibition of the CRISPR-Cas system.

specifically inhibit only the Type I-E/I-C systems. From this perspective, the possibility remains that the AcrIE7 preferentially interacts with ssDNA exposed by the R-loop due to additional interactions with specific Type I-E/I-C Cascades. Based on our experimental results, we proposed a model in which AcrIE7 binds to the ssDNA exposed by R-loop formation, preventing Cas3 from cleaving the DNA. However, we have not directly confirmed that AcrIE7 binds to ssDNA within the Cascade system. Such confirmation would be an important future research topic to further clarify our model. Although further research is required to understand the evolutionary and specific benefits of this inhibition strategy, it represents an intriguing addition to the repertoire of Acr-mediated CRISPR-Cas inhibition.

Methods

The structure of AcrIE7 was solved by Sel-MET SAD phasing. For EMSA, reactions were prepared with either AcrIE7 or mutant AcrIE7, combined with 42 bp dsDNA or 42 bp ssDNA. The ssDNA cleavage inhibition assay was conducted by incubating AcrIE7 or its mutants with 50 nM 6-FAM-labeled ssDNA. The detail methods are described in *SI Appendix*.

Data, Materials, and Software Availability. The coordinate and structure factor have been deposited into the Protein Data Bank under the code of 9KJB (16). All study data are included in the article and/or *SI Appendix*.

ACKNOWLEDGMENTS. This work was supported by a Brain Korea 21 FOUR through the National Research Foundation funded by the Ministry of Education of Korea.

1. R. Barrangou *et al.*, CRISPR provides acquired resistance against viruses in prokaryotes. *Science* **315**, 1709–1712 (2007).
2. A. L. Borges, A. R. Davidson, J. Bondy-Denomy, The discovery, mechanisms, and evolutionary impact of anti-CRISPRs. *Annu. Rev. Virol.* **4**, 37–59 (2017).
3. H. G. Hampton, B. N. J. Watson, P. C. Fineran, The arms race between bacteria and their phage foes. *Nature* **577**, 327–336 (2020).
4. W. Sun *et al.*, AcrIIC4 inhibits type II-C Cas9 by preventing R-loop formation. *Proc. Natl. Acad. Sci. U.S.A.* **120**, e2303675120 (2023).
5. G. E. Kim, H. H. Park, AcrIIA28 is a metalloprotein that specifically inhibits targeted-DNA loading to SpyCas9 by binding to the REC3 domain. *Nucleic Acids Res.* **52**, 6459–6471 (2024).
6. L. Liu, M. Yin, M. Wang, Y. Wang, Phage AcrIIA2 DNA mimicry: Structural basis of the CRISPR and anti-CRISPR arms race. *Mol. Cell* **73**, 611–620 e613 (2019).
7. D. Ka, S. Y. An, J. Y. Suh, E. Bae, Crystal structure of an anti-CRISPR protein, AcrIIA1. *Nucleic Acids Res.* **46**, 485–492 (2018).
8. C. N. Trost *et al.*, An anti-CRISPR that pulls apart a CRISPR-Cas complex. *Nature* **632**, 375–382 (2024).
9. Y. Kim *et al.*, Anti-CRISPR AcrIIC3 discriminates between Cas9 orthologs via targeting the variable surface of the HNH nuclease domain. *FEBS J.* **286**, 4661–4674 (2019).
10. N. D. Marino *et al.*, Discovery of widespread type I and type V CRISPR-Cas inhibitors. *Science* **362**, 240–242 (2018).
11. A. Pawluk *et al.*, Disabling a type I-E CRISPR-Cas nuclease with a bacteriophage-encoded anti-CRISPR protein. *mBio* **8**, e01751-17 (2017).
12. J. Bondy-Denomy *et al.*, Multiple mechanisms for CRISPR-Cas inhibition by anti-CRISPR proteins. *Nature* **526**, 136–139 (2015).
13. K. E. Watters *et al.*, Potent CRISPR-Cas9 inhibitors from *Staphylococcus* genomes. *Proc. Natl. Acad. Sci. U.S.A.* **117**, 6531–6539 (2020).
14. D. Y. Kim, S. Y. Lee, H. J. Ha, H. H. Park, Structural basis of Cas3 activation in type I-C CRISPR-Cas system. *Nucleic Acids Res.* **52**, 10563–10574 (2024).
15. L. M. Leon, A. E. Park, A. L. Borges, J. Y. Zhang, J. Bondy-Denomy, Mobile element warfare via CRISPR and anti-CRISPR in *Pseudomonas aeruginosa*. *Nucleic Acids Res.* **49**, 2114–2125 (2021).
16. D. Y. Kim, H. H. Park, Crystal structure of Anti-CRISPR AcrIF7. Protein Data Bank (PDB). https://www.rcsb.org/structure/unreleased/9KJB. Deposited 12 November 2024.